Nuclear actin cable with multiple branches during yeast meiosis

Tomoko Takagi[1, 2, 3], Masako Osumi[2, 4] and Akira Shinohara[1]*

[1]Institute for Protein Research, Osaka University, Suita, Osaka 565-0871, Japan
[2]Laboratory of Electron Microscopy and [3]Department of Chemical and Biological Sciences, Japan Women's University, Tokyo 112-8681, Japan
[4]NPO: Integrated Imaging Research Support, Tokyo102-0093, Japan

Running title: Nuclear F-actin during meiosis

Keyword: Meiosis, actin cables, F-actin, nuclei

*Corresponding author
Akira Shinohara
Mailing address:
Institute for Protein Research, Osaka University,
3-2 Yamadaoka, Suita, Osaka 565-0871 JAPAN
Phone: 81-6-6879-8624
FAX: 81-6-6879-8626
E-mail: ashino@protein.osaka-u.ac.jp
ORCID: 0000-0003-4207-8247

Abstract

Actin polymerizes to form filaments/cables for motility, transport, and structural framework in a cell. Recent studies show that actin polymers are present not only in cytoplasm, but also in nuclei of vertebrate cells, and their formation is induced in response to stress. Here, by electron microscopic observation with rapid freezing and high-pressure freezing, we found a unique polymerized form of actin inside of nuclei of budding yeast cells undergoing meiosis. The nuclear actin cable during meiosis consists of several actin filaments with a rectangular lattice arrangement and is associated with multiple branched cables/filaments showing "feather-like" appearance. The cable is immuno-labeled with anti-actin antibody and sensitive to an actin-depolymerizing drug. Like cytoplasmic actin cables, nuclear actin cables are rarely seen in pre-meiotic cells and spores, and are induced during meiotic prophase-I. We speculate that nuclear actin cables play a role in nuclear events during meiotic prophase I.

Introduction

In the cytoplasm, as a cytoskeletal protein, actin polymerizes to form a filament (F-actin) for various cellular functions such as motility, division, phagocytosis, endocytosis, and membrane trafficking [1]. Dynamics of cytoplasmic actin filaments are highly regulated by various factors in different environments. Actin is also present in nuclei [2]. Actin monomer functions as a component of several chromatin-remodeling complexes for transcription [3].

Recent studies showed that polymerized forms of actin are present in nuclei of various types of vertebrate and invertebrate cells [4-9]. About forty-years ago, Fukui and his colleagues identified actin bundles in *Dictyostelium* and HeLa cells upon the treatment with dimethyl sulfoxide [10-12]. In *Xenopus* oocytes, nuclear actin forms a mesh of filaments, which is involved in the protection of nucleoli from gravity-induced aggregation [13]. In starfish oocytes, actin filaments promote the breakdown of nuclear envelope and, by forming a mesh, the capture of chromosomes by spindles in cell division [14]. In mouse oocytes, actin filaments promote chromosome segregation during meiosis I and II [5]. Somatic mammalian cells induce the formation of actin polymers transiently in a nucleus in response to stress; serum starvation, heat shock, and DNA damage such as DNA double-strand breaks (DSBs). For serum starvation, the F-actin is involved in transcription by helping the activity of a transcriptional cofactor, MRTF (myocardin-related transcription factor) [15, 16]. Nuclear F-actin also promotes repair of DSBs in mammalian and fruit fly cells [4, 7, 17].

In budding and fission yeasts, actin is present in the cytoplasm as a polymerized form such as rings, patches and cables [18-20] as well as less-defined structures called filasome [21]. In budding yeast *Saccharomyces cerevisiae*, actin cables in cytoplasm play a role in the transport in mitotic budded cells. Previous electron microscopic (EM) analysis of cytoplasm in fixed mitotic cells revealed a linear actin bundle containing multiple actin filaments [22]. Actin cables/bundles and some other actin-filament associated structures are also visualized by using a green fluorescent protein (GFP) fused with an actin-binding protein, Abp140, or by staining with an actin-specific peptide with a fluorescent dye such as phalloidin [23].

Actin filaments/cables are present also in of the cytoplasm of meiotic

yeast cells [24, 25]. The actin cables are induced to form during meiotic prophase-I (meiotic G2 phase) and form a network that surrounds the nucleus. It is proposed that meiosis-specific motion of telomeres on the nuclear envelope is mediated by "Piggy-Back" mechanism, in which cytoplasmic actin cables attached to NE drives the motion of telomeres, thus chromosomes through protein ensembles embedded in NE [24, 26]. Previous EM observation of a nucleus of chemically fixed cells undergoing meiosis showed synaptonemal complex (SC), a meiosis-specific chromosome structure as well as nuclear microtubules from Spindle pole body (SPB), a yeast centrosome [27-29]. However, it still remains less known about ultra-structure such as cytoskeletons including actin cables inside of yeast cells during meiosis.

In this study, we analyzed ultra-structures inside meiotic yeast cells, particularly an actin-associated structure called actin cables, by using freeze-substitution electron microscope [30]. As expected, meiotic prophase-I cells induce the formation of cytoplasmic actin cables. Interestingly, we also detected actin cables inside nuclei in cells undergoing meiosis I, but not in pre-meiotic cells or spores. The structure of nuclear actin cables is similar to that in the cytoplasm of meiotic cells. The cables are immuno-labeled with anti-actin antibody and are sensitive to the treatment with an actin-depolymerizing drug. Meiosis-specific nuclear actin cables consist of multiple actin filaments with a regular arrangement and show multiple branches. These results indicate that actin cables or actin cable-networks are formed inside nuclei of cells undergoing chromosomal events in prophase-I; e.g. recombination, chromosome motion and the SC formation. The biological implications of nuclear actin cables in meiotic cells are discussed.

Results

Electron microscopic observation of meiotic yeast cells

Previous analysis of actin localization in budding yeast by staining with phalloidin and live-cell imaging using a GFP-fusion of Abp140 revealed that, during prophase of meiosis I, yeast cells contain actin cables in cytoplasm [2, 25, 26]. To get more detailed ultra-structures of cytoskeletons and its spatial relationship

with organelles inside of meiotic yeast cells, we used a transmission electron microscope (TEM). Cells were quickly frozen, and substituted with the fixative and stained with osmium (freeze-substitution method) [30]. Thin sections of cells were observed under TEM (Fig. 1). With the freeze-substitution method, cellular organelles including nucleus, mitochondrion, and vacuoles in cytoplasm filled with dense-stained ribosomes were well preserved (Fig. 1a, c, f, j). The nucleus was surrounded with double-layered nuclear membranes and contained electron-dense regions, which corresponds with nucleolus (Fig. 1b). During meiosis prophase-I, i.e. 4 h after the induction of meiosis by incubating cells with sporulation medium, nuclei contact vacuoles forming nuclear-vacuole junctions (NVJ; Fig. 1f) as shown previously [31]. At 8 h, four pre-spore cells were formed inside of the cells (Fig. 1j).

Nuclear actin cables in yeast meiosis

Previous EM analyses of mitotic cells of both budding and fission yeasts have shown three distinct actin sub-cellular structures; rings, cables, and patches in addition to filasome and amorphous structure [18-21]. We could detect a cable structure in cytoplasm during meiotic prophase-I (Fig. 1f, g, i). This cable contains actin since immuno-gold labeling using anti-actin antibody showed that gold particles were seen on the cables in cytoplasm (Fig. 2a). Thus, we called the structure as “actin cable” hereafter. Previous EM analysis detected similar cytoplasmic actin cables in mitotic yeast cells [22] and later immuno-EM confirmed the presence of actin cables [32]. We also detected gold particles on less electron dense areas in cytoplasm, which might correspond to filasomes (see also Fig. 2a’), a novel actin-containing membrane-less sub-cellular structure in cytoplasm originally found in fission yeast [21]. The filasome may differ from actin patches involved in endocytosis. Consistent with previous cytological studies of actin [24, 25], actin cables in cytoplasm are rarely seen in pre-meiotic cells at 0 h (in G1 or G0 phases; Fig. 1a and 3a for quantification) and 2 h (in S-phase, Fig.1c), but are observed in cells at 4 h after the induction of meiosis (Fig. 1f and 3a). The formation of the cable in cytoplasm peaks at 5 h, which corresponds with late prophase-I and gradually decreases during further progression of meiotic divisions (Fig. 3a). In some cases, cytoplasmic actin cables are located near

mitochondria (Fig.1i). Among the sections, we rarely saw the attachment of cytoplasmic actin cables to the nucleus, although a previous cytological study suggested that cytoplasmic actin cables attach to the NE [24].

In addition to cytoplasmic actin cables, we detected the similar cables inside of nuclei of meiotic cells (Fig. 1c, d, e, f, h). The structure of cables in nuclei is similar to that in cytoplasm (compare Fig. 1g and 1h). This cable is structurally different from microtubules in the nucleus emanating from Spindle Pole body (SPB: see Fig. 6). Importantly, immuno-gold labeling using anti-actin antibody showed gold labels on these cables in nuclei as those in cytoplasm (Fig. 2b), indicating that the nuclear cable contains actin. Thus, we referred a cable containing actin in nuclei to as “nuclear actin cable”.

Previously, the treatment of meiotic cells with an actin-depolymerizing chemical, Latrunculin B (LatB), largely reduced cytoplasmic actin cables [24, 25]. To confirm that the cables in nuclei as well as in cytoplasm are indeed formed through actin polymerization, we treated 4-h meiotic yeast cells with LatB for 1 h and examined the presence of actin cables in cells under EM. As shown in Fig. 2c, after the treatment with LatB, the number of cables (a section positive to actin cables) is greatly reduced in nuclei (60% [1/12, 12/22, 15/22, 25/32] at 4 h for positive nucleus to 31% [8/14, 3/21]) after 1 h-treatment; P=0.0247, Fisher’s exact test) without affecting nuclear microtubules. This indicates that the nuclear cable is sensitive to LatB, supporting the idea that cables in nucleus, like those in cytoplasm, are formed through actin polymerization.

Nuclear actin cables are formed during prophase-I

We checked the presence of nuclear actin cables in different stages of meiosis (Fig. 3a). As a control, we measured nuclei containing microtubules. The nuclear microtubules are seen at 0 h and sections positive to microtubules are increased slightly during meiotic prophase-I. Nuclear actin cables appear earlier during meiosis than cytoplasmic cables (Fig. 3a). At 0 h before the induction of meiosis in which most of cells are G1, we detected few cables in nuclei (Fig. 1a; 0/10, 1/10 and 1/34 cells in three independent time courses) as well as in cytoplasm (1/10, 1/22 and 1/34 cells). Few cables were also found in four nuclei of pre-spore cells, suggesting that the cables disassemble by the formation of

pre-spore cells (Fig. 1j). Kinetic analysis revealed that nuclear actin cables were seen at 2 h post-induction of meiosis (Fig. 1c, d), when 40% (13/31, 8/22) of sectioned cells contained nuclear actin cables, indicating the formation of the structure is an early event of meiosis; e.g. during pre-meiotic S-phase. At 4 h, actin cable-positive nuclei were observed with 60% frequency (1/12, 12/22, 15/22, 25/32). Cells in late prophase-I at 5 h showed a peak in both actin cable-positive nuclei and cytoplasm (Fig. 4a). After 6 h both nuclear and cytoplasmic actin cables were decreased (Fig. 4c). At 6 h, when about a half of the cells enter in meiosis I, we detected the cables in a bridge-like structure between two nuclei undergoing anaphase-I (Fig. 4b). This suggests that the actin cables passed into the daughter nuclei during meiosis I division.

Nuclear actin cables form branches

Both actin cables in cytoplasm and nuclei are structurally similar. The cables contain three to ten thin parallel filaments and exhibit multiple branched filaments, which look like “feather” (Fig. 1g, h). Cross-sections of the nuclear cables often reveal a regular rectangular/square arrangement (lattice) of filaments with repeated units of alternate single and double filaments (Fig. 1e; shown as red dots in Fig.1e’). From a long cable, additional cables/filaments seem to form a branch (Fig. 1e, g, h). At this resolution some branched filaments look attached directly to filaments in a main cable while the other filaments are not.

The diameter of the thin filament in nuclear actin cables is around 7-8 nm (Fig. 3c; mean±S.D.=8.3±1.3 nm [n=17], 7.1±1.1 nm [n=8], 7.6±1.0 nm [n=13] for three independent sections), which roughly corresponds with the size of a single yeast actin filament reconstituted *in vitro* [33, 34]. An average distance between adjacent filaments (Supplementary Fig. 1) is ~15nm (Fig. 3d; mean±S.D.=15.2±3.1 nm [n=50], 8.3±3.2 nm [n=10], 12.2±2.5 nm [n=42]). The length of the cables varies from 50 nm up to 1,000 nm, near the diameter of the nucleus (Fig. 3b). The length of nuclear actin cables in sections (Fig. 3b; mean±S.D.=306±223 nm [n=60], median=274 nm) is not different from that in cytoplasm (mean±S.D.=304±179 nm [n=121], median=238 nm; *P*=0.64, Mann-Whitney’s *U*-test). In some cases, actin cables span across through whole

nucleus (~1 μm, see also, Fig. 7). The longer actin cable consists of multiple short cables, rather than a single linear cable (see Fig. 4a and 7-5).

As with branched cables, we measured an angle between main actin cables and branched cables/filaments (Fig. 5). At 4 h, angles between the main cable and branched filaments are 25°-40° with sub-peak of 15°-20° (Fig. 3e; mean±S.D.=38°±19° [n=31], median=34°). These values are quite different from an angle of branches of actin filament mediated by Arp2/3 complex with a value of 70° [35]. We also noticed branches from a single actin cable are oriented same direction, suggesting the presence of the directionality of the cable.

To get more spatial information on nuclear actin cables, we checked serial sections of a nucleus in yeast cells at 4 h in meiosis (Fig. 6 and 7). To achieve in-depth freezing in samples, we froze cells under a high pressure [36]. With high-pressure freezing specimens suitable for sectioning were obtained. Importantly, we did not see any change of sub-cellular structures including actin cables in yeast cells prepared by rapid freezing or high-pressure freezing (compare Fig. 1 with Fig. 6 and 7). We often detected multiple “feather-like actin structures” in different sections (Fig. 6), indicating that actin cables are an abundant nuclear structure. In some sections, a long cable that spans entire nucleus is observed (Fig. 7-5 and 7-6), and the end of the cable is likely attached to the nuclear envelope (Fig. 7; arrows in Fig. 7-6).

Nuclear actin cables by chemical fixation

Yeast cells are surrounded with thick cell walls, which impair penetration of staining reagents such as osmic tetroxide. We also stained spheroplasted meiotic yeast cells with osmic acid after fixation with glutaraldehyde (without any freezing, Supplementary Fig. 2) and, in some cases, prepared serial sections for EM observation (Supplementary Fig. 3). With this procedure, the mitochondria are contrasted highly (Supplementary Fig. 2). Membrane structures such as nuclear membrane were partially deformed, possibly due to hypo-osmotic conditions. Importantly, even under this condition, we could detect actin cables in both the nucleus and the cytoplasm of cells during meiotic prophase-I (Supplementary Fig. 2d, e, g). Observation of serial sections revealed that actin cables attach to the inner nuclear membrane (Supplementary Fig. 3).

Discussion

In this study, by using TEM with rapid freezing-fixation, we found nuclear actin cables in budding yeast cells undergoing the physiological program of meiosis. We could also detect actin cables in cytoplasm, which are induced during prophase I [24]. Since we used rapid freezing to preserve structures inside of cells, it is unlikely that the actin cable is an artifact produced by sample preparation, which might be induced by external stress and/or fixation. Moreover, we also detect the actin cables in nuclei fixed with chemicals without freezing (Supplementary Fig. 2 and 3).

Both nuclear and cytoplasmic actin cables consist of multiple parallel filaments. This is consistent with previous EM analyses showing cytoplasmic actin cables in fixed mitotic cells, which are present as a linear cable of multiple filaments [22]. On the other hand, the actin cables formed during meiosis appear to have a unique ultra-structure: a single actin cable exhibits multiple lateral branches of filaments (Fig. 8). Some branched filaments are directly attached to filaments in main cables while the other filaments are not (Fig. 8a). This branch structure is different from a branch of actin filament from a single actin filament, which is seen in cytoplasm in moving edges of various vertebrate cells and is mediated by the Arp2/3 complex. In yeast, branched “short” actin filaments (not cables) are often associated with mitotic actin patches that mediate endocytosis [20]. More recently, it is shown that, in mammalian cells, Arp2/3 controls the formation of nuclear F-actin in response to DSBs [7]. The angle between the Arp2/3-dependent branched filaments is ~70° [35]. On the other hand, angles in the meiotic nuclear actin cables are ~35°. Moreover, meiotic nuclear actin cables do not show a single branch of the filament, but rather showed a branch of the cables with multiple filaments, suggesting a unique branching mechanism for nuclear actin cables in the yeast. Therefore, the actin cables with multiple branches in yeast meiotic nuclei are a unique polymerized form of actin (Fig. 8c).

Nuclear (and cytoplasmic) actin cables seem to contain a unique arrangement of actin filaments, in which alternate pattern of 1 and 2 filaments is observed in a cross section of the cables (Fig. 8a and b). This alternate pattern provides rectangular/square arrangement of filaments in a single cable. The

distance of inter-filaments is mainly 10-15 nm. *In vitro* biochemical reconstitution of actin cables with an actin-bundling protein, fimbrin, showed packing of the filaments with 12 nm inter-filament distance [37-39]. Thus, the formation of actin cables in meiotic nuclei might be mediated by a fimbrin-like actin-binding protein. Budding yeast contain multiple actin-bundling proteins; Sac6/fimbrin, Scp1, lpg1, Crn1 and Abp140 [20]. Among them, fimbrin/Sac6 is a major protein for actin bundling, which plays a critical role in bundling the filaments in cytoplasmic actin cables in mitotic cells. *In vitro* reconstitution of actin bundles in the presence of human fimbrin shows an arrangement of actin filaments in a hexagonal lattice [39]. This arrangement is similar to *in vivo* arrangement in terms of a unit of equilateral triangle. However, in meiotic nuclear actin cables, rather hexagonal, tetragonal lattice is observed in which two sides are required for the self-assembly of filaments in the lattice and the others are for branch formation. In muscle, actin filaments exhibit tetragonal lattice in the Z-band of adjacent sarcomeres [40, 41]. In this case, α-actinin seems to mediate inter-filament interaction. It has been reported that fission yeast, but not budding yeast, contain α-actinin-like protein [42, 43]. It is interesting to find an α-actinin-like protein in budding yeast.

The average length of nuclear actin cables is 300-400 nm, which is slightly shorter than the cables which form a contracting ring in fission yeast [18, 44]. Nuclear actin cables are able to elongate up to 1 μm (Fig. 3b and Fig. 7). This long cable consists of a few cables in a linear array, rather than a single cable. We speculate that some branched actin cables are assembled into a long cable. Several actin cables are present in a single nucleus of meiotic cells (Fig. 6 and 7), indicating that nuclear actin cables are abundant. Nuclear actin cables are induced from very early meiotic prophase-I such as 2-h post induction of meiosis and are present to at least by meiosis I nuclear division. Actin cables are abundant not only in nuclei, but also in cytoplasm particularly during late prophase-I (Fig. 4a). On the other hand, we rarely see nuclear or cytoplasmic actin cables in a G1 cell (pre-meiotic) or in spores (Fig. 1a, i).

Recent studies in mammalian cultured cells demonstrate the presence of a polymerized form actin in nuclei, which can be detected with a fluorescence probe such as Life-ACT [17] or directly by EM [12]. The nuclear F-actin formation is

induced in response to stress such as serum starvation, heat, and DNA damage [8]. The nuclear F-actin is involved in the gene expression, the relocation of chromosomal loci as well as DNA repair [4, 7, 17]. Like mammalian cells, meiotic actin cable formation in meiotic prophase-I yeast cells may appear in response to DNA damage, since meiotic cells are programed to induce multiple DNA DSBs [45]. However, during meiosis, the formation of nuclear actin cables starts at 2 h post-induction of meiosis, prior to DSB formation, which begins at 3 h, suggesting that nuclear actin cable formation might not be associated with DSB formation during yeast meiosis. Therefore, we need more analysis to know relationship between nuclear actin cables and meiotic DSB formation/repair.

Actin polymerization, thus the formation of actin cables, in cytoplasm is involved in chromosome motion during prophase-I in budding yeast [26]. Cytoplasmic actin cables promote meiotic chromosome motion through SUN-KASH protein ensembles in the NE [46] since the motion is sensitive to the LatB. We speculate that actin cables may form three-dimensional structure through branching the cables inside of meiotic nuclei. Our results here suggest that nuclear actin cables also plays a role in the movement of meiotic chromosomes. Alternatively, nuclear actin cables may protect nuclear structures from external forces generated during meiosis as seen in *Xenopus* oocyte [13], by providing a rigid structure that resists mechanical stress. To distinguish functional differences between actin cables in nuclei and cytoplasm, we need to develop techniques that inactivate either only nuclear or only cytoplasmic actin polymerization without affecting the role of actin monomer of chromatin remodeling complex in nuclei.

Acknowledgements

We thank Drs. N. Nagata and I. Mabuchi for discussion and suggestions. We also thank members of the Laboratory of Electron Microscopy, Japan Women's University and Ms. Y. Osaki in NPO: Integrated Imaging Research Support. We thank Drs. Gasser, Hurst, Shimada, Mabuchi, Yasunaga, and Usukura for critical reading of the manuscript. This work was supported by JSPS KAKENHI Grant Number: 22125001, 22125002, 15H05973 and 16H04742 to A.S and by the Open Research Center of JWU established in private universities in Japan with

the support of the Ministry of Education, Culture, Sports, Science and Technology to M. O.

Author contributions

TT, MO, and AS conceived and designed the experiments. TT performed the all EM experiments. TT and AS analyzed the data. TT, MO, and AS prepared the manuscript.

Competing interests

The authors declare no competing interests.

Materials and Methods

Strains and culture

S. cerevisiae SK1 diploid strain, MSY832/833 (*MAT*α*/MAT****a****, ho::LYS2/", lys2/", ura3/", leu2::hisG/", trp1::hisG/"*), was used for meiotic time course.

Yeast cell culture and time-course analyses of the events during meiosis and the cell cycle progression were performed as described previously [47, 48]. Briefly, 1 ml of diploid yeast culture in YPAD was cultured in 200 ml of SPS media for 16 h. Cells were collected and, after washing with H_2O, were re-suspended in 200 ml of SPM media (20 mM KCH_3COO, 0.02% raffinose) to start meiosis.

Rapid Freezing for transmission electron microscopy

Specimens for freeze-substitution electron microscopy were prepared according to previously described method [49, 50], with slight modifications. Cells were harvested by centrifugation. The cell pellets were sandwiched between two copper disks (3 mm in diameter). Specimens were quickly frozen with liquid propane using a rapid freezing device (KF80; Leica, Vienna, Austria). Specimens were freeze-substituted in cold absolute acetone containing 2% osmium tetroxide (OsO_4) at –80°C for 48-72 h and were then warmed gradually (at -40°C for 4 h, at -20°C for 2 h, at 4°C for 2 h and at room temperature for 2 h) and washed with absolute acetone and rinsed with QY-2. Substitution for embedding was infiltrated with Quetol-812 mixture (10, 30, 50, 70, 80 and 90

and 100% pure resin). The specimens polymerized at 60°C for 2 days.

High pressure freezing fixation for transmission electron microscopy

The specimens for high-pressure freeze-substitution electron microscopy were prepared according to previously described method [51] with slight modifications. The pelleted cells were pipetted into aluminum specimen carriers (Leica) and frozen in a high-pressure freezing machine HPM-010 (BAL-TEC, Liechtenstein). The cells were transferred to 2% OsO_4 in cold absolute acetone. Substitution fixation was carried out at −90°C for over 80 h. After the fixation, the specimens were warmed gradually (at -40°C for 2 h, at -20°C for 2 h, at 4°C for 2 h and at room temperature for 1 h) and washed with absolute acetone and then with exchange to 0.1% uranyl acetate in absolute acetone. After the staining, samples were washed with absolute acetone and rinsed with QY-2. Substitution and embedding were described in above.

EM grid preparation and observation

Specimens for morphological observation were sectioned using a ULTRACUT-S ultramicrotome (Reichert-Nissei, Tokyo, Japan). Ultrathin sections were cut with thickness of 50-60 nm and mounted on copper grids. Specimens for immuno-staining were mounted on nickel grids. Ultrathin sections were stained with 4% uranyl acetate for 12 min in dark at room temperature and citrate mixture (SIGMA-ALDRICH) for 2 min at room temperature, and examined using JEM-1200EXS at 120kV or JEM-1400 transmission electron microscope (JEOL, Tokyo, Japan) at 100 kV.

Immunoelectron Microscopy and Immunolabelling

For immuno-electron microscopy, chemical fixation samples shown below were etched with 1% H_2O_2 for 5min at room temperature. Otherwise, cell pellets were sandwiched between two aluminum disks (diameter 3 mm). And specimens were quickly frozen with liquid propane. They were freeze-substituted in cold absolute acetone containing 0.01% OsO_4. Substitution took place for 48-72 h at -80°C, and were then warmed gradually (at -40°C for 4 h, at -20°C for 2h and at 4°C for 1h) and washed with dehydration ethanol at 4°C. Then the cells were

washed twice with cold ethanol and substituted at 4°C and infiltration was done in the LR white and ethanol mixture (10, 30, 50, 70, 80, 90, 100% pure resin). Specimens were embedded in pure resin and polymerized at 50°C for 1-2 days.

Immunolabelling was carried out by previously described method [51] with a slight modification. The sections mounted on nickel grids were incubated with chromatographically purified goat IgG (Zymed Laboratories, Inc., San Francisco, USA) diluted in blocking buffer, 0.1% bovine serum albumin (Sigma Chemical Co., St. Louis, USA) in 50 mM TBS (137 mM NaCl, 2.7 mM KCl, 50 mM Tris-HCl; pH 7.5), to 1/30 concentration for 30 min at room temperature. Affinity-purified mouse anti-actin monoclonal antibodies (MAB1501: Chemicon International Inc., Temecula, USA) diluted in blocking buffer to 1/100 concentration were applied to the sections, incubated for 1 h at room temperature. The sections were washed with blocking buffer. Goat antibodies to mouse IgG labeled with 10 nm colloidal gold (British BioCell International, Cardiff, UK) diluted in blocking buffer to 1/40 concentration and applied to sections for 1 h at room temperature. Sections were washed with blocking buffer and running water. The sections were stained with 4% aqueous uranyl acetate and citrate mixture (Sigma Chemical Co., St. Louis, USA).

Latrunculin B treatment

After cultured in SPM medium for four hours, cells were treated with 30 μM Latrunculin B (R&D Systems) dissolved in 0.1% DMSO at 30°C for 1 hour. After the post-treatment, cells were collected and fixed by the rapid freezing mentioned later.

Chemical fixation method for electron microscopy

Cells for chemical fixation were shaking-cultured for 4 hours in SPM containing 1 M sorbitol (SPMS) at 130 rpm and 30°C, details described above. Specimens for chemical fixation were shaking-cultured for 4 hours in SPM containing 1 M sorbitol (SPMS) at 130 rpm 30°C, details described above. Cells were treated for 2 min with 0.2 M DTT in ZK buffer (25 mM Tris-HCl and 0.8 M KCl). Then cells were treated for 30min with 0.5 mg ml^{-1} Zymolyase 100T (Seikagaku Corp., Tokyo) in ZK buffer at room temperature. And cells treated with 0.5% Triton

X-100 dissolved in PEM (20 mM PIPES, 20 mM $MgCl_2$, 10 mM EGTA, pH 7.0), protease inhibitors, and 1 M sorbitol for permeabilization in the presence of 4.2 μM phalloidin (Sigma-Aldrich) for 1 min, these treatments were performed as described previously [18, 44].

Specimens for TEM were prepared as described previously [21, 44, 52, 53]. Briefly, harvested cells were fixed with 2% glutaraldehyde (Electron Microscope Sciences) and 0.2% tannic acid (TAAB) for 1 h at 4°C. After washings with PEM, cells were post-fixed in 2% OsO_4 in PEM for 1 h at 4°C. After washed out with D.W., cells were embedded in 2% agarose and cut into blocks smaller than 1 mm^3. And then, samples were dehydrated with ethanol series (50%, 70%, 80%, 90%, 95%, 99.5%, and Super Dehydrated ethanol). Samples rinsed with QY-2. Gradually increase the concentration of the resin infiltrated with Quetol-812 (Nisshin EM, Tokyo) mixture (10, 30, 50, 70, 80, 90 and 100% pure resin).

Image processing and measurement

Measurement of diameter of actin cables and distance between actin cables was carried out using ImageJ (NCBI, https://imagej.nih.gov/ij/).

Statistics

Statistical significance for Length of actin cables between that in nucleus and cytoplasm was analyzed using the Mann-Whitney's *U*-test. The null hypothesis was that there exists no variation of the length between nucleus and cytoplasm.

Statistical significance for existence of actin cables in cells with and without LatB treatment was analyzed using Fisher's exact test. The null hypothesis was that LatB treatment did not affect existence of actin cables in cells. Two-sided *P*-value was shown.

References

1. Pollard, T.D., Blanchoin, L. & Mullins, R.D. Molecular mechanisms controlling actin filament dynamics in nonmuscle cells. *Annual review of biophysics and biomolecular structure* **29**, 545-576 (2000).
2. Hurst, V., Shimada, K. & Gasser, S.M. Nuclear Actin and Actin-Binding Proteins in DNA Repair. *Trends in cell biology* (2019).
3. Kapoor, P. & Shen, X. Mechanisms of nuclear actin in chromatin-remodeling complexes. *Trends in cell biology* **24**, 238-246 (2014).
4. Caridi, C.P. *et al.* Nuclear F-actin and myosins drive relocalization of heterochromatic breaks. *Nature* **559**, 54-60 (2018).
5. Mogessie, B. & Schuh, M. Actin protects mammalian eggs against chromosome segregation errors. *Science (New York, N.Y.)* **357** (2017).
6. Philimonenko, V.V., Janacek, J., Harata, M. & Hozak, P. Transcription-dependent rearrangements of actin and nuclear myosin I in the nucleolus. *Histochemistry and cell biology* **134**, 243-249 (2010).
7. Schrank, B.R. *et al.* Nuclear ARP2/3 drives DNA break clustering for homology-directed repair. *Nature* **559**, 61-66 (2018).
8. Virtanen, J.A. & Vartiainen, M.K. Diverse functions for different forms of nuclear actin. *Current opinion in cell biology* **46**, 33-38 (2017).
9. Zhang, S., Kohler, C., Hemmerich, P. & Grosse, F. Nuclear DNA helicase II (RNA helicase A) binds to an F-actin containing shell that surrounds the nucleolus. *Experimental cell research* **293**, 248-258 (2004).
10. Fukui, Y. Intranuclear actin bundles induced by dimethyl sulfoxide in interphase nucleus of *Dictyostelium*. *J Cell Biol* **76**, 146-157 (1978).
11. Fukui, Y. & Katsumaru, H. Nuclear actin bundles in Amoeba, Dictyostelium and human HeLa cells induced by dimethyl sulfoxide. *Experimental cell research* **120**, 451-455 (1979).
12. Fukui, Y. & Katsumaru, H. Dynamics of nuclear actin bundle induction by dimethyl sulfoxide and factors affecting its development. *J Cell Biol* **84**, 131-140 (1980).
13. Samwer, M. *et al.* The nuclear F-actin interactome of *Xenopus* oocytes

reveals an actin-bundling kinesin that is essential for meiotic cytokinesis. *The EMBO journal* **32**, 1886-1902 (2013).

14. Feric, M. & Brangwynne, C.P. A nuclear F-actin scaffold stabilizes ribonucleoprotein droplets against gravity in large cells. *Nature cell biology* **15**, 1253-1259 (2013).
15. Baarlink, C., Wang, H. & Grosse, R. Nuclear actin network assembly by formins regulates the SRF coactivator MAL. *Science (New York, N.Y.)* **340**, 864-867 (2013).
16. Panayiotou, R. *et al.* Phosphorylation acts positively and negatively to regulate MRTF-A subcellular localisation and activity. *eLife* **5** (2016).
17. Belin, B.J., Lee, T. & Mullins, R.D. DNA damage induces nuclear actin filament assembly by Formin -2 and Spire-(1/2) that promotes efficient DNA repair. [corrected]. *eLife* **4**, e07735 (2015).
18. Kamasaki, T., Arai, R., Osumi, M. & Mabuchi, I. Directionality of F-actin cables changes during the fission yeast cell cycle. *Nature cell biology* **7**, 916-917 (2005).
19. Kobori, H., Yamada, N., Taki, A. & Osumi, M. Actin is associated with the formation of the cell wall in reverting protoplasts of the fission yeast *Schizosaccharomyces pombe*. *Journal of cell science* **94 (Pt 4)**, 635-646 (1989).
20. Moseley, J.B. & Goode, B.L. The yeast actin cytoskeleton: from cellular function to biochemical mechanism. *Microbiology and molecular biology reviews : MMBR* **70**, 605-645 (2006).
21. Takagi, T., Ishijima, S.A., Ochi, H. & Osumi, M. Ultrastructure and behavior of actin cytoskeleton during cell wall formation in the fission yeast *Schizosaccharomyces pombe*. *Journal of electron microscopy* **52**, 161-174 (2003).
22. Adams, A.E. & Pringle, J.R. Relationship of actin and tubulin distribution to bud growth in wild-type and morphogenetic-mutant *Saccharomyces cerevisiae*. *J Cell Biol* **98**, 934-945 (1984).
23. Yang, H.C. & Pon, L.A. Actin cable dynamics in budding yeast. *Proc Natl Acad Sci U S A* **99**, 751-756 (2002).
24. Koszul, R., Kim, K.P., Prentiss, M., Kleckner, N. & Kameoka, S. Meiotic

chromosomes move by linkage to dynamic actin cables with transduction of force through the nuclear envelope. *Cell* **133**, 1188-1201 (2008).

25. Taxis, C. *et al.* Dynamic organization of the actin cytoskeleton during meiosis and spore formation in budding yeast. *Traffic* **7**, 1628-1642 (2006).
26. Koszul, R. & Kleckner, N. Dynamic chromosome movements during meiosis: a way to eliminate unwanted connections? *Trends in cell biology* **19**, 716-724 (2009).
27. Byers, B. & Goetsch, L. Electron microscopic observations on the meiotic karyotype of diploid and tetraploid *Saccharomyces cerevisiae*. *Proc Natl Acad Sci U S A* **72**, 5056-5060 (1975).
28. Moens, P.B. & Rapport, E. Spindles, spindle plaques, and meiosis in the yeast Saccharomyces cerevisiae (Hansen). *J Cell Biol* **50**, 344-361 (1971).
29. Zickler, D. & Olson, L.W. The synaptonemal complex and the spindle plaque during meiosis in yeast. *Chromosoma* **50**, 1-23 (1975).
30. Osumi, M. Visualization of yeast cells by electron microscopy. *Journal of electron microscopy* **61**, 343-365 (2012).
31. Tsai, I.T. *et al.* Interorganelle interactions and inheritance patterns of nuclei and vacuoles in budding yeast meiosis. *Autophagy* **10**, 285-295 (2014).
32. Mulholland, J. *et al.* Ultrastructure of the yeast actin cytoskeleton and its association with the plasma membrane. *J Cell Biol* **125**, 381-391 (1994).
33. Greer, C. & Schekman, R. Actin from Saccharomyces cerevisiae. *Molecular and cellular biology* **2**, 1270-1278 (1982).
34. Kilmartin, J.V. & Adams, A.E. Structural rearrangements of tubulin and actin during the cell cycle of the yeast *Saccharomyces*. *J Cell Biol* **98**, 922-933 (1984).
35. Mullins, R.D., Heuser, J.A. & Pollard, T.D. The interaction of Arp2/3 complex with actin: nucleation, high affinity pointed end capping, and formation of branching networks of filaments. *Proc Natl Acad Sci U S A* **95**, 6181-6186 (1998).
36. Osumi, M., Konomi, M., Sugawara, T., Takagi, T. & Baba, M.

High-pressure freezing is a powerful tool for visualization of Schizosaccharomyces pombe cells: ultra-low temperature and low-voltage scanning electron microscopy and immunoelectron microscopy. *Journal of electron microscopy* **55**, 75-88 (2006).

37. Hanein, D., Matsudaira, P. & DeRosier, D.J. Evidence for a conformational change in actin induced by fimbrin (N375) binding. *J Cell Biol* **139**, 387-396 (1997).
38. Hanein, D. *et al.* An atomic model of fimbrin binding to F-actin and its implications for filament crosslinking and regulation. *Nature structural biology* **5**, 787-792 (1998).
39. Volkmann, N., DeRosier, D., Matsudaira, P. & Hanein, D. An atomic model of actin filaments cross-linked by fimbrin and its implications for bundle assembly and function. *J Cell Biol* **153**, 947-956 (2001).
40. Burgoyne, T., Morris, E.P. & Luther, P.K. Three-Dimensional Structure of Vertebrate Muscle Z-Band: The Small-Square Lattice Z-Band in Rat Cardiac Muscle. *Journal of molecular biology* **427**, 3527-3537 (2015).
41. Luther, P.K. Three-dimensional reconstruction of a simple Z-band in fish muscle. *J Cell Biol* **113**, 1043-1055 (1991).
42. Virel, A. & Backman, L. Molecular evolution and structure of alpha-actinin. *Molecular biology and evolution* **21**, 1024-1031 (2004).
43. Wu, J.Q., Bahler, J. & Pringle, J.R. Roles of a fimbrin and an alpha-actinin-like protein in fission yeast cell polarization and cytokinesis. *Mol Biol Cell* **12**, 1061-1077 (2001).
44. Kamasaki, T., Osumi, M. & Mabuchi, I. Three-dimensional arrangement of F-actin in the contractile ring of fission yeast. *J Cell Biol* **178**, 765-771 (2007).
45. Keeney, S., Giroux, C.N. & Kleckner, N. Meiosis-specific DNA double-strand breaks are catalyzed by Spo11, a member of a widely conserved protein family. *Cell* **88**, 375-384 (1997).
46. Conrad, M.N. *et al.* Rapid telomere movement in meiotic prophase is promoted by NDJ1, MPS3, and CSM4 and is modulated by recombination. *Cell* **133**, 1175-1187 (2008).
47. Shinohara, M., Gasior, S.L., Bishop, D.K. & Shinohara, A. Tid1/Rdh54

promotes colocalization of Rad51 and Dmc1 during meiotic recombination. *Proceedings of the National Academy of Sciences of the United States of America* **97**, 10814-10819 (2000).

48. Shinohara, M., Sakai, K., Ogawa, T. & Shinohara, A. The mitotic DNA damage checkpoint proteins Rad17 and Rad24 are required for repair of double-strand breaks during meiosis in yeast. *Genetics* **164**, 855-865 (2003).
49. Baba, M. & Osumi, M. Transmission and scanning electron microscopic examination of intracellular organelles in freeze-substituted Kloeckera and *Saccharomyces cerevisiae* yeast cells. *J. Electron Microsc. Tech.* **5**, 249-261 (1987).
50. Yamaguchi, M., Okada, H. & Namiki, Y. Smart specimen preparation for freeze substitution and serial ultrathin sectioning of yeast cells. *Journal of electron microscopy* **58**, 261-266 (2009).
51. Humbel, B.M. *et al.* In situ localization of beta-glucans in the cell wall of *Schizosaccharomyces pombe*. *Yeast (Chichester, England)* **18**, 433-444 (2001).
52. Naito, N., Yamada, N., Kobori, H. & Osumi, M. Contrast enhancement by ruthenium tetroxide for observation of the ultrastructure of yeast cells. *J. Electron Microsc. Tech.* **40**, 416-419 (1991).
53. Osumi, M. *et al.* Dynamics of cell wall formation in fission yeast, Schizosaccharomyces pombe. *Fungal genetics and biology : FG & B* **24**, 178-206 (1998).

Figure legends.

Figure 1. EM images of meiotic yeast cells

a, b TEM images of a yeast diploid cell at 0 h. The samples were prepared with freeze-fixation and sectioned. Magnified image is shown in (b). Bars indicate 1 μm and 500 nm in (a) and (b), respectively.

c-e. TEM images of a yeast diploid cell at 2 h after incubation with SPM. Magnified views are shown in (d, e). (d) vertical-sectioned of actin filaments are shown by an arrow. (e) cross-sections of actin filaments are shown by arrows (left) and marked by red dots (right). Bars indicate 1 μm (c) and 100 nm (d, e).

f-i. TEM images of a yeast diploid cell at 4 h after incubation with SPM. A whole cell (f) and magnified views of boxed region with actin cables in cytoplasm (g) and in nucleus (h), where cables of feather-like actin filaments (arrows) are seen. An actin cable (arrow) is seen near mitochondorion (i). Bars indicate 1 μm (f) and 100 nm (g, h and i).

j. TEM image of a yeast diploid cell at 8 h after incubation with SPM. Bars indicate 1 μm. ER, endoplasmic reticulum; L, Lipid body; M, mitochondrion; N, nucleus; NM, nuclear membrane (envelope); Nu, nucleolus; NVJ, nuclear-vacuole junction; SW, spore wall; V, vacuole.

Figure 2. Nuclear cables contain actin and its formation depends on actin polymerization

a, b. Immuno-gold labeling using anti-actin antibody was carried out as described in Materials and Methods. Images of actin cables in cytoplasm (a) and in nucleus (b) in a cell at 4 h are shown. The positions of gold particles are shown in arrowheads. Dotted circles were actin patches (a'). The area surrounded by dotted line shows a nucleus (b'). The positions of gold particles are marked by yellow dots (a' and b').

c, d. TEM image of a Latrunculin B-treated cell (c) and nucleus (d). Cells were incubated with SPM for 4 h and treated with Latrunculin B for 1 h. The samples were prepared by rapid-freezing with fixation and sectioned. Bars indicate 1 μm. L, Lipid body; M, mitochondrion; N, nucleus; NM, nuclear

membrane; Nu, nucleolus; MTs, microtubules.

Figure 3. Quantification of nuclear and cytoplasmic actin cables during meiosis.

a. Kinetics of the formation of actin cables in nuclei (red) and cytoplasm (green) as well as nuclear microtubules (blue) at different time of meiosis. A number of sections containing actin cables were counted and % of actin-positive nuclei and –cytoplasm as well as microtubule-positive nuclei are shown.

b. Distribution of lengths of actin cables in nuclei and cytoplasm at 4 h in meiosis. The length of actin cables in a cross-section were measured and ranked every 50 nm. The number of actin cables in nuclei (red) and cytoplasm (green) in each rank in three independent images is shown.

c. Distribution of a diameter of actin filaments in nuclei at 4 h in meiosis. The diameter of actin filaments in a cross-section were measured and ranked every 2 nm. The number of each rank in three independent images is shown in different colors.

d. Distribution of a distance between two adjacent actin filaments in nuclei (red) and cytoplasm (green) at 4 h in meiosis. The distance between two adjacent actin filaments in a cross-section were measured and ranked every 2 nm. The number of each rank in three independent images is shown in different colors.

e. Distribution of angles of actin branches in nuclei at 4 h in meiosis. An angle between actin cables and branched actin cables was measured. The angles were ranked every 5 degree. The number of each rank is shown.

Figure 4. EM images of meiotic yeast cells during mid-prophase I.

a-c. TEM images of a yeast diploid cell after incubation with SPM for 5 h (a) and 6 h (b, c). The samples were prepared by rapid-freezing with fixation and sectioned. Black arrows indicate actin cables. Bars indicate 500 nm. M, mitochondrion; MTs, microtubules; N, nucleus; NM, nuclear membrane (envelope); Nu, nucleolus; V, vacuole.

Figure 5. EM images of actin cables showing branches

a, b. Representative images of nuclear actin cables. a', b'. Representative lines for the angle measurement are shown in red.

Figure 6. EM images of serial sections of yeast nucleus during mid-prophase I

Samples were prepared by high-pressure freezing as described in Materials and Methods. Serial sectioned TEM images of a single cell at 4 h are shown. White and black arrows indicate spindle microtubules and actin cables, respectively. Double black arrows indicate cytoplasmic actin cables. Bar indicates 500 nm. M, mitochondrion; NM, nuclear membrane; NP, nuclear pore; SPB, spindle pole body ; V, vacuole; Ves, Vesicle.

Figure 7. EM images of serial sections of yeast nucleus during mid-prophase I

Serial sectioned TEM images of a cell at 4 h, which were fixed with high-pressure freezing, are shown. Black double arrows indicate actin cables, which is likely to attach to nuclear envelop. Bar indicates 500 nm. M, mitochondrion; NM, nuclear membrane; Nu, nucleolus; L, Lipid body; V, vacuole.

Figure 8. A model of actin cables with branches.

A schematic representation of actin cables (red) with multiple branches (blue) is shown. Schematic presentation of a cross-section of a nuclear actin cable (a); arrangement of actin filaments in the cable (b); lateral view of actin cables (c).

Supplementary Figures

Supplementary Figure 1. EM images of actin cables for measurement of diameter and inter-filament distance

A representative image of actin cables is shown (a) with a reference line for the measurement of an inter-filament distance (blue, b) and of a diameter (red, c). Bar indicates 200 nm.

Supplementary Figure 2. EM images of chemically fixed meiotic yeast cells in mid-prophase I

TEM images of a yeast diploid cell after incubation with SPM for 0 h (a, b), 4 h (c, d, e), and 6 h (f, g). The samples were fixed with chemicals (glutaraldehyde and OsO_4) and sectioned. Magnified images with actin cable in nucleus (b, d, e, g) and in cytoplasm (c) are shown. Bars indicate 1 μm (a, c, f) and 100 nm (b, d, e, g). M, mitochondrion; N, nucleus; NM, nuclear membrane; V, vacuole. Arrows indicate actin cables.

Supplementary Figure 3. Serially sectioned EM images of a chemically fixed yeast cell in mid-prophase I

Serial sectioned TEM images of an identical cell at 4 h, cells were fixed with chemicals (glutaraldehyde and OsO_4). Bar indicates 500 nm. Arrows indicate actin cables.

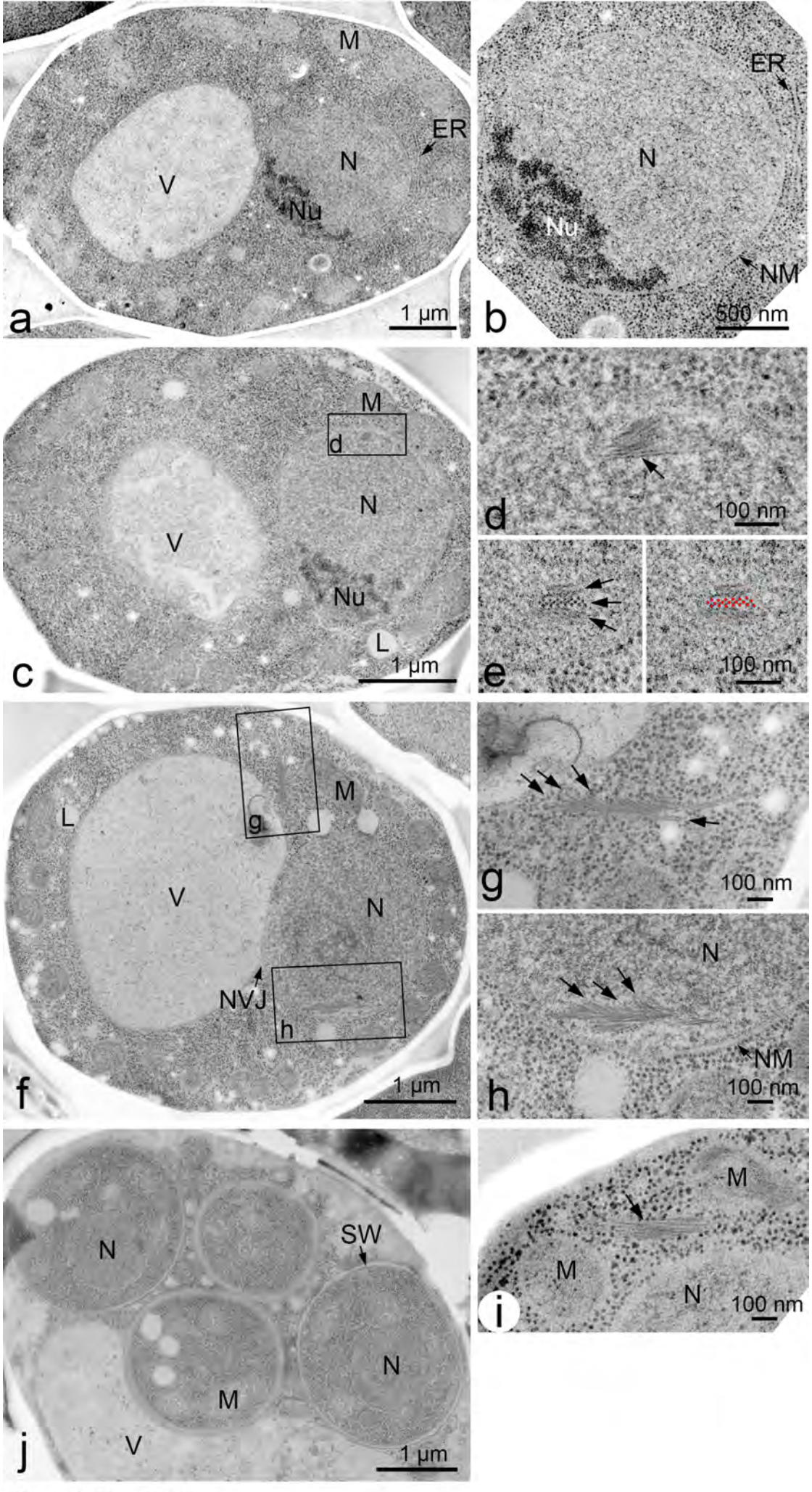
M
ER
N
V
Nu
a
1 μm
ER
N
Nu
NM
b
500 nm
M
d
N
V
Nu
L
c
1 μm
d
100 nm
e
100 nm
L
M
g
V
N
NVJ
h
f
1 μm
g
100 nm
N
NM
h
100 nm
N
SW
N
M
V
j
1 μm
M
M
N
i
100 nm

Fig. 1 Takagi

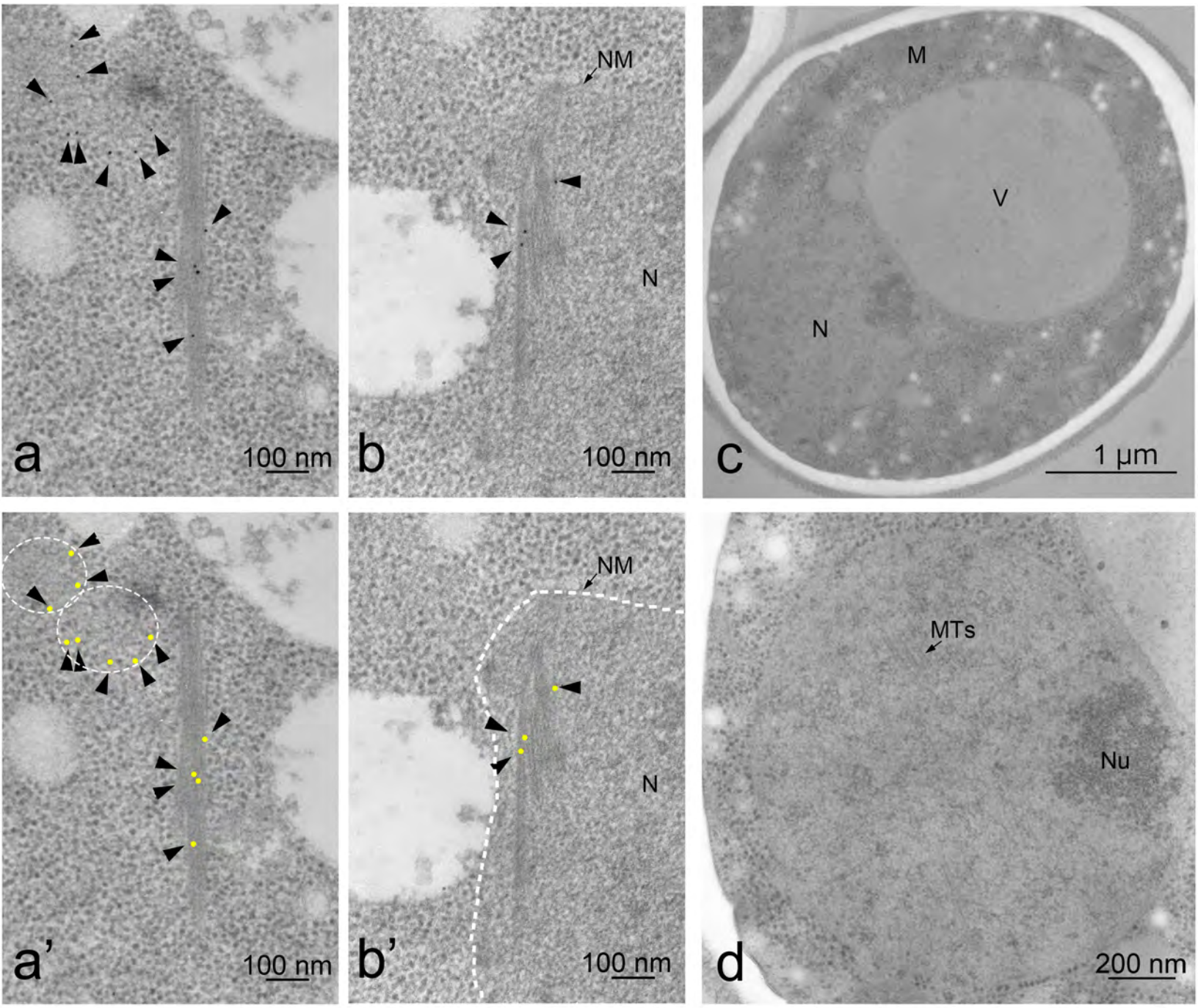

Fig. 2 Takagi

Figure 3. Takagi

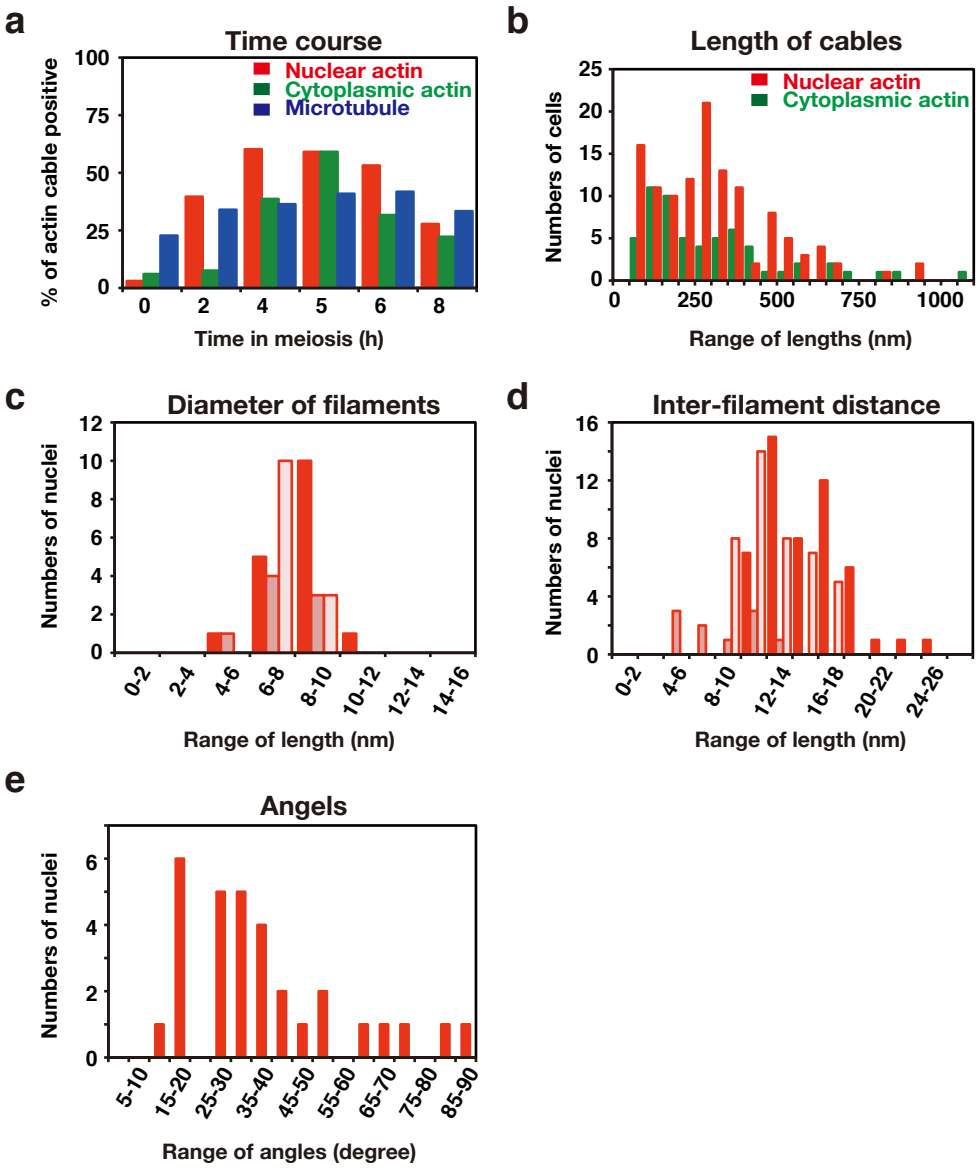

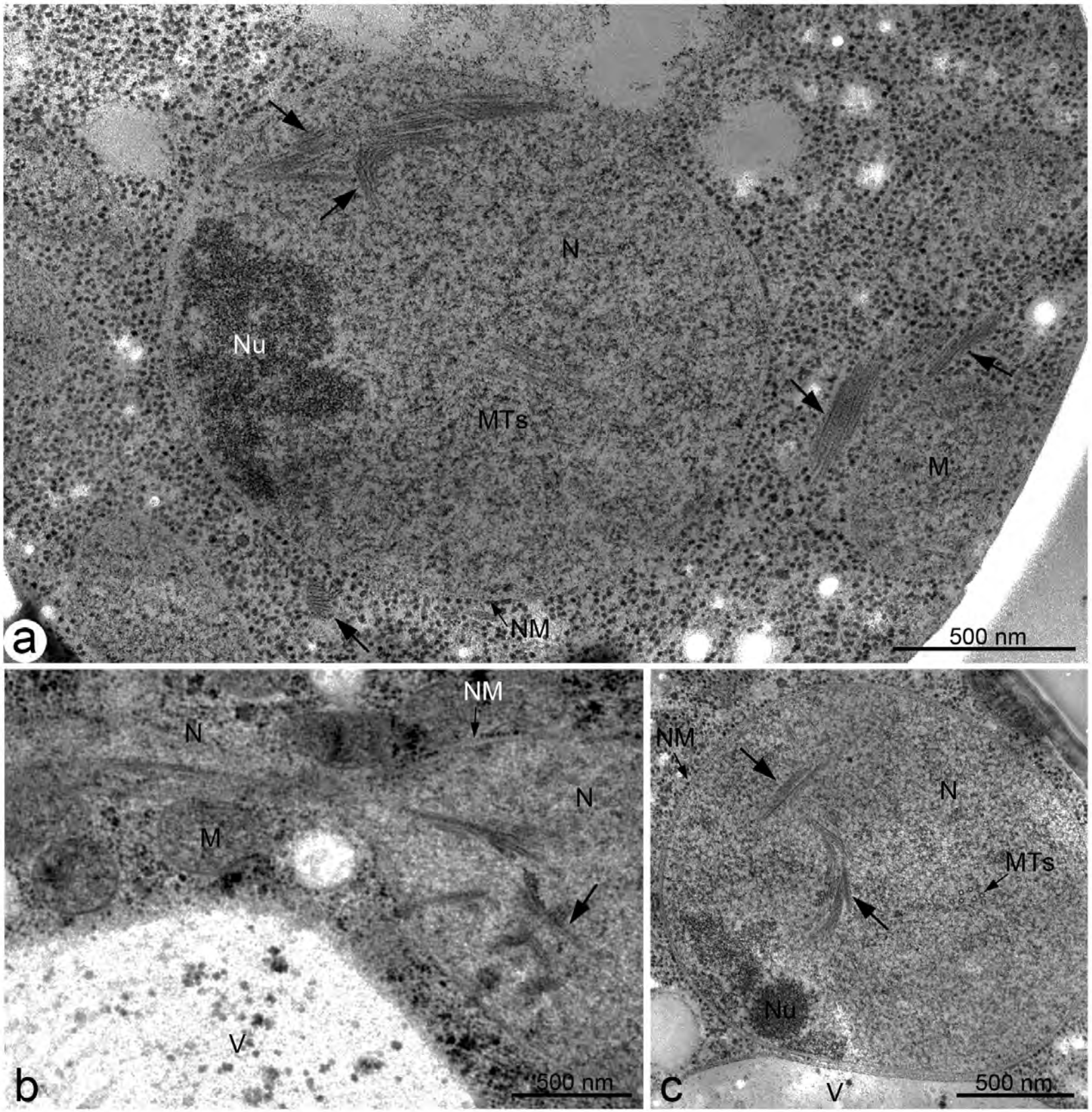

Fig.4 Takagi

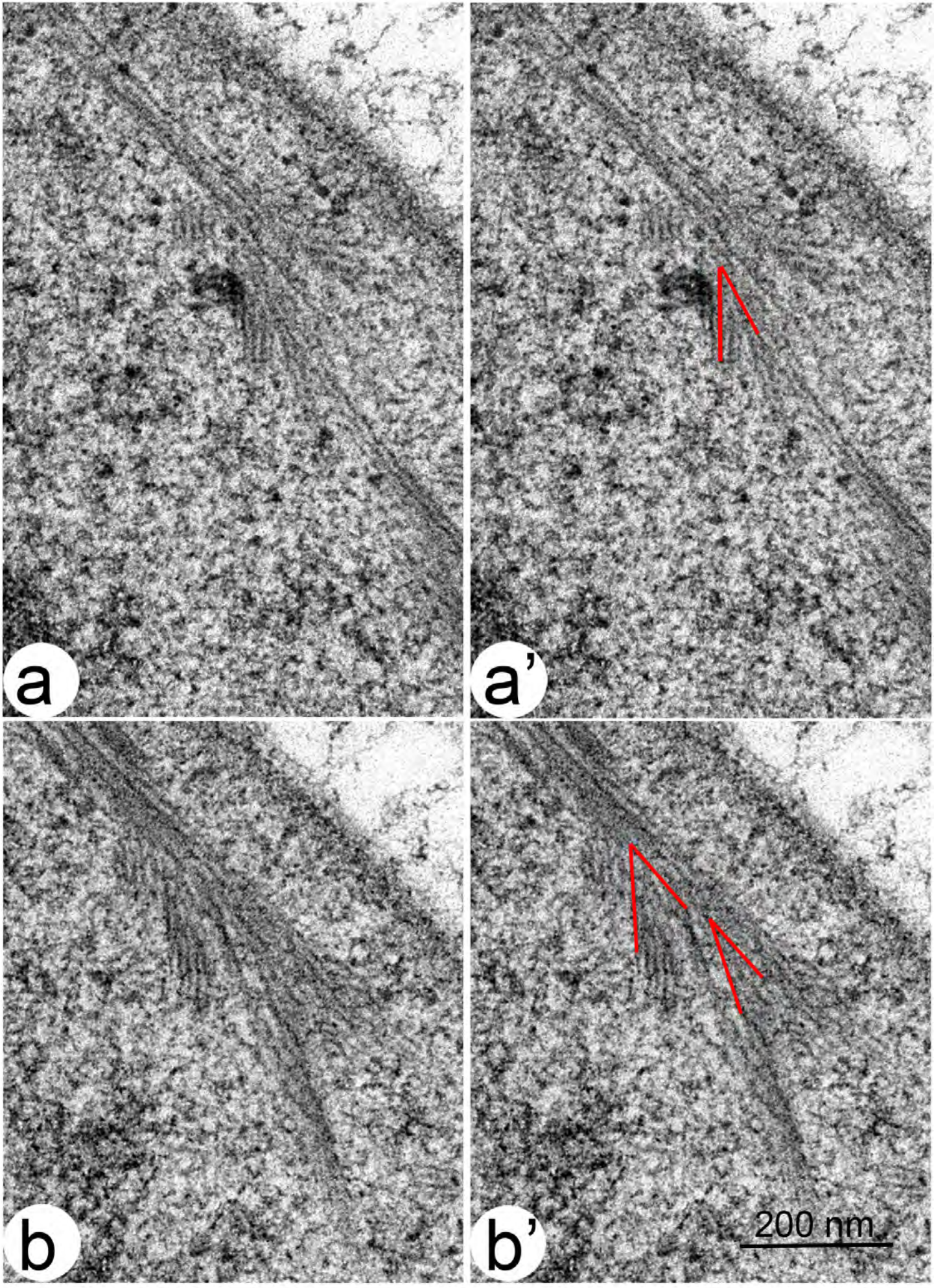

Fig. 5 Takagi

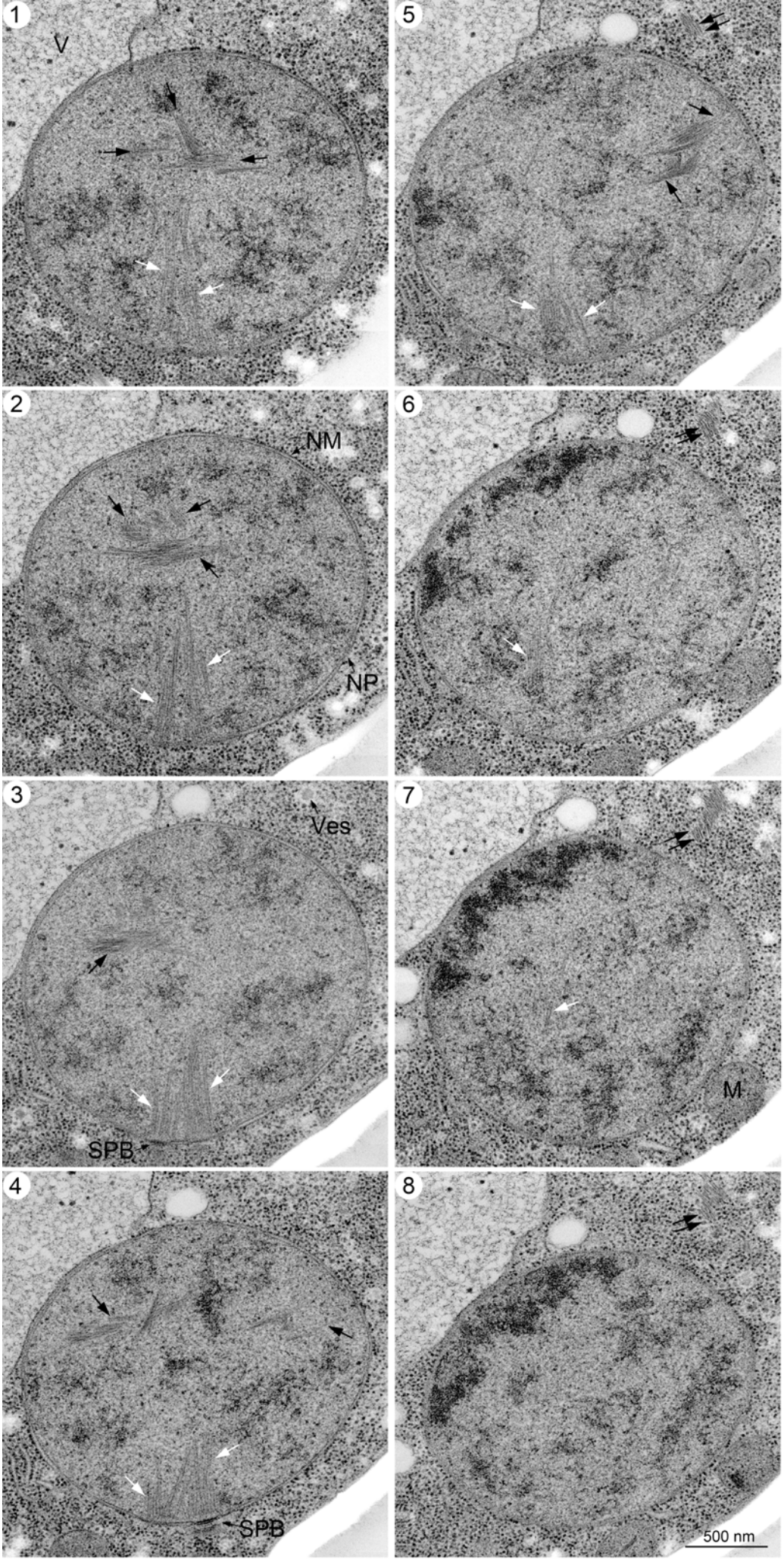

Fig. 6 Takagi

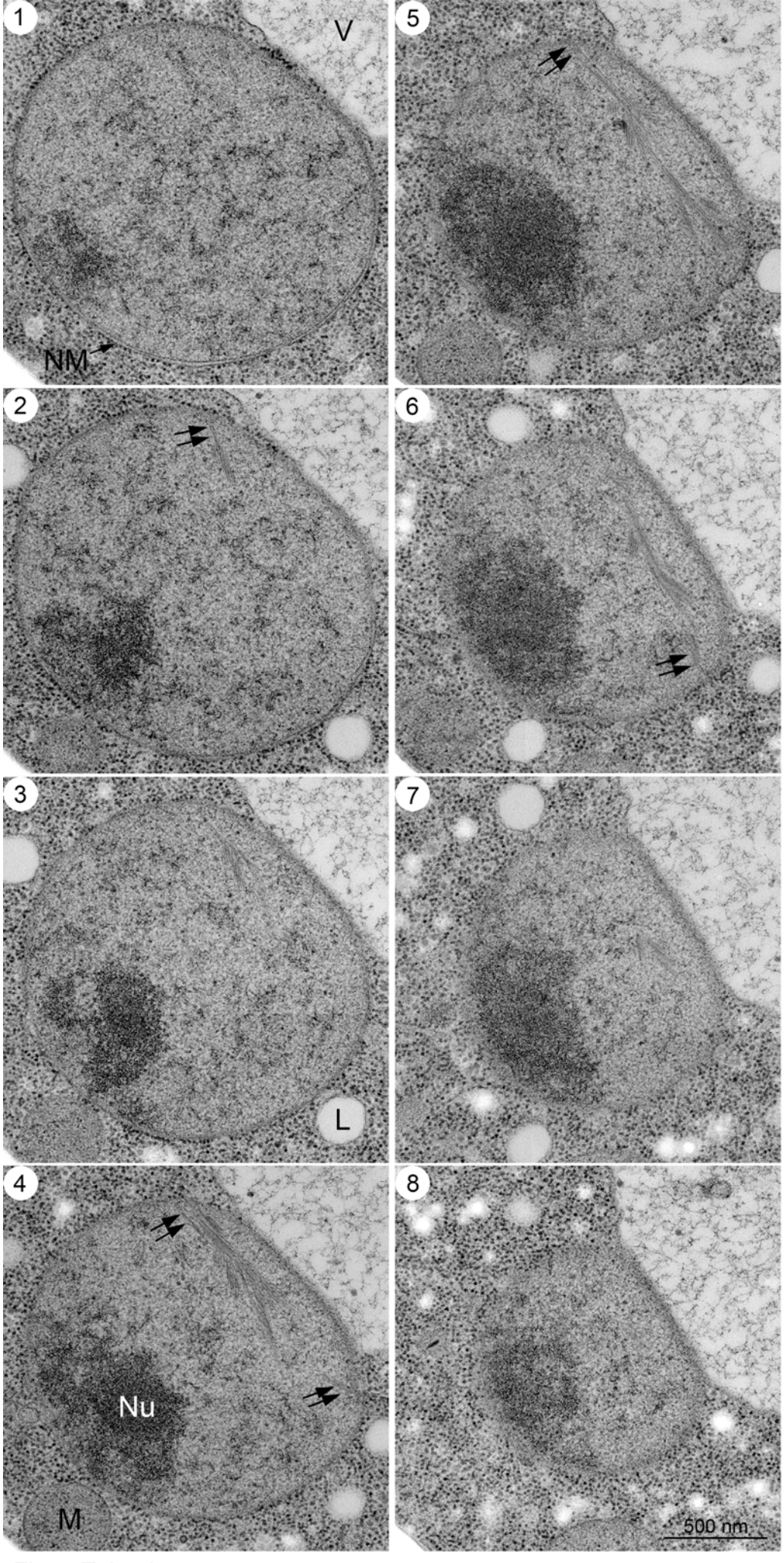

Fig. 7 Takagi

Fig. 8 Takagi

a

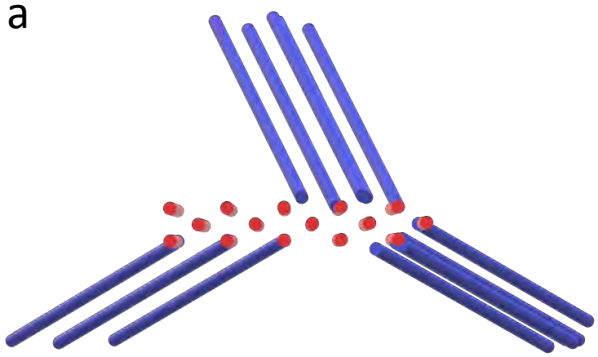

b

c

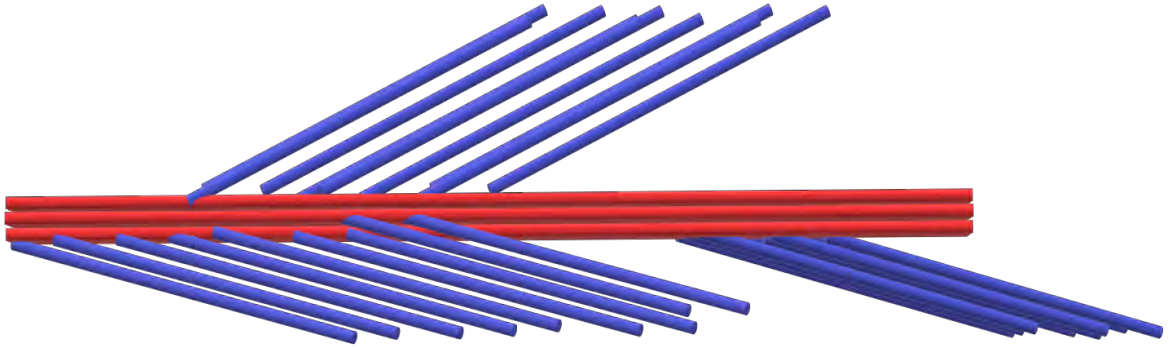

Supplemtary Figure 1. Takagi

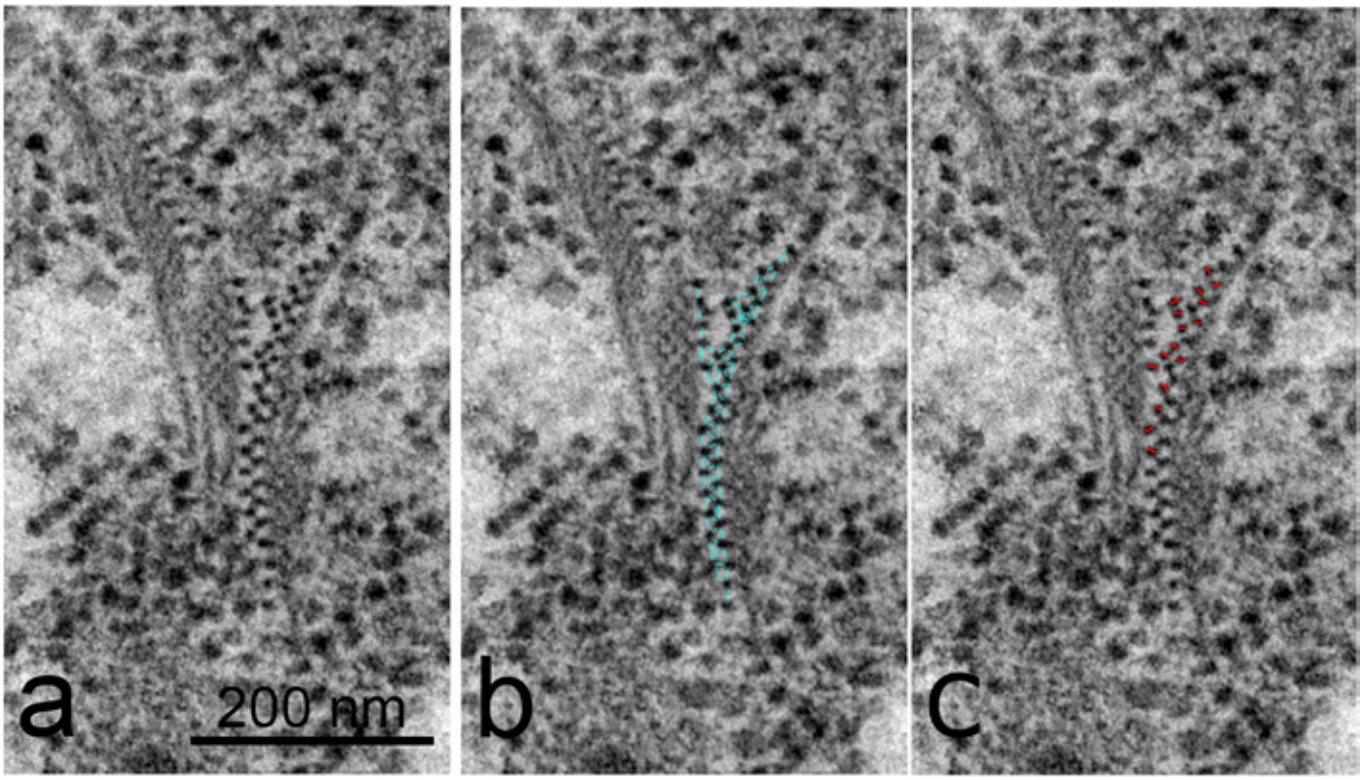

Supplementary Figure 2. Takagi

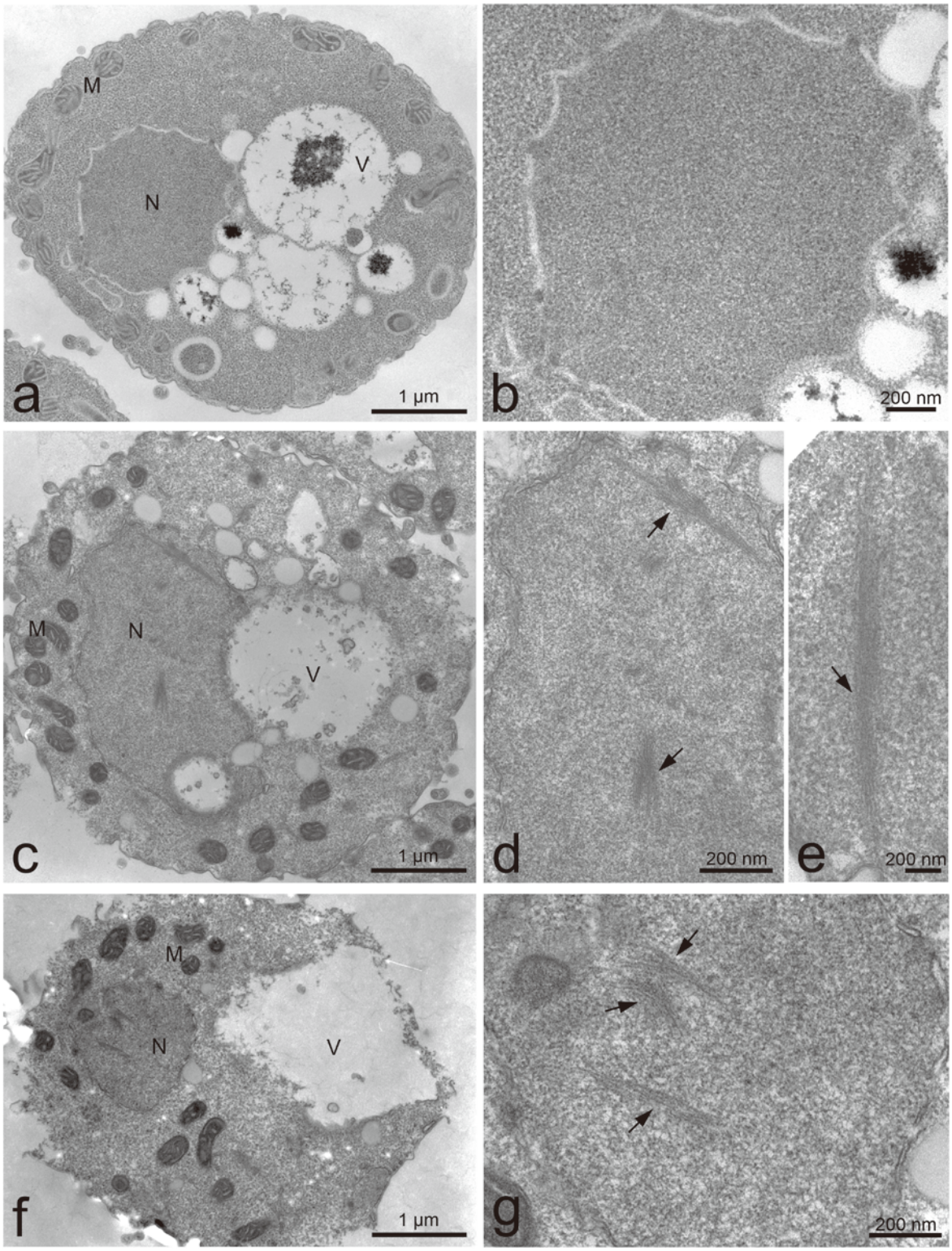

Supplementary Figure 3. Takagi